JPEDAV (2005) 26:452-457
DOI: 10.1361/154770305X66510
1547-7037/$19.00 ©ASM International

Tracer Diffusion of Niobium and Titanium in Binary and Ternary Titanium Aluminides

Sergiy V. Divinski, Christian Klinkenberg, and Christian Herzig

(Submitted July 19, 2005)

This study presents recent results on titanium (Ti) and niobium (Nb) diffusion in binary (α_2-Ti_3Al and γTiAl) and ternary high-Nb-containing (γTiAl-10Nb) Ti aluminides. Three different techniques were used to measure self-diffusion and solute (Nb) diffusion. The radiotracer technique combined with mechanical sectioning by grinding was applied at higher temperatures, whereas ion-beam sputtering or secondary ion mass spectrometry was used to analyze the short penetration profiles at lower temperatures. The results measured by these different techniques for different penetration depths are very consistent. Nb is a slower diffuser compared to Ti in the ternary as well as in the binary Ti aluminides. The heavy alloying of γTiAl with 10at.% Nb, however, enhances significantly both the Ti and the Nb diffusivities. The diffusion mechanisms for Ti and Nb in ordered Ti aluminides are discussed.

1. Introduction

Titanium (Ti) aluminides are attractive materials for high-temperature structural applications such as turbocharger wheels or gas turbine blades. Alloying is frequently used to improve their physical properties. Heavy alloying with niobium (Nb) was especially found to yield a large gain in the mechanical properties[1,2] and the oxidation resistance[3,4] of the Ti aluminides. Therefore, research on Ti aluminides has recently focused on high-Nb-containing TiAl alloys.[5]

Many important mechanical and physical properties of the structural alloys, especially at elevated temperatures, are related to atomic self-diffusion. For example, the superior creep resistance of high-Nb-containing TiAl alloys was established,[2] which might hypothetically be explained by decreased diffusion rates in TiAlNb.

To give an additional insight into the physical nature of the improved creep resistance of high-Nb-containing Ti aluminides, the diffusion behavior of binary and ternary Ti aluminides has to be elucidated. In this article, the authors review recent results on Ti self-diffusion and Nb solute diffusion in the binary (α_2-Ti_3Al and γTiAl) and the ternary TiAl-Nb titanium aluminides. According to the ternary phase diagram for the Ti-Al-Nb system,[6] the Ti-54Al-10Nb alloy lies in the γ phase field.

This article is a revised version of the paper printed in the *Proceedings of the First International Conference on Diffusion in Solids and Liquids—DSL-2005*, Aveiro, Portugal, July 6-8, 2005, Andreas Öchsner, José Grácio and Frédéric Barlat, eds., University of Aveiro, 2005.

Sergiy V. Divinski and **Christian Herzig,** Institut für Materialphysik, Universität Münster, Wilhelm-Klemm-Str. 10, D-48149 Münster, Germany; and **Christian Klinkenberg,** Niobium Products Company GmbH, Steinstr. 28, D-40210 Düsseldorf, Germany. Contact e-mail: divin@uni-muenster.de.

2. Experimental Details

2.1 Sample Preparation

Alloys were prepared in the group of Dr. F. Appel at the Gesellschaft zur Kernenergieverwertung in Schiffbau und Schiffahrt (GKSS) Research Center, Geesthacht, Germany. Pure elements (Ti of 99.99 wt.% purity, Al of 99.999 wt.% purity, and Nb of 99.9 wt.% purity) were typically used to produce the binary (α_2-Ti_3Al and γTiAl) or ternary (γTi-54Al-10Nb) alloys by repeated induction heat melting. The alloys with the compositions Ti-33at.%Al, Ti-56at.%Al, and Ti-54at.%Al-10at.%Nb were used in the present investigation. The complete results on self-diffusion (Ti) and Nb solute diffusion in α_2-Ti_3Al and γTiAl were published[7-10] as a function of the composition of the corresponding phases.

The ingots were cut into discs of about 2 to 3 mm in thickness and about 8 mm in diameter by spark erosion. After a standard polishing procedure, the samples were annealed under high-vacuum conditions (10^{-6} Pa) above the intended diffusion annealing temperature to eliminate possible surface stresses and to reduce the dislocation density of the material.

The diffusion samples were placed in sealable compact TiAl containers wrapped with a Ta foil. This prevents preferred Al evaporation from the specimen surface. The final composition of the alloys was determined by electron microprobe analysis.

2.2 Diffusion Study

Ti diffusion was studied by applying the ^{44}Ti radioisotope (68 and 78 keV γ radiation; half-life 47.3 years). The radioisotope was either evaporated in a vacuum chamber on the prepared surface of the specimen or was dropped directly (as an aqueous solution of Ti chloride [$TiCl_4$]) and dried. Tracer deposition by evaporation was applied in the case of short diffusion penetration profiles to satisfy instan-

taneous source initial conditions. The detected initial amount of the radioisotope on the sample surface was about 1 to 2 kBq.

On the other hand, it is a quite involved task to measure reliably the diffusion rate of the ^{95}Nb radioisotope.[11] The radioisotope ^{95}Nb (766 keV γ radiation; half-life 35 d) was available only in radiochemical equilibrium with its mother nuclide, ^{95}Zr (757 keV γ radiation; half-life 65.5 d). Therefore, the concentration of ^{95}Nb in a given section of a specimen is determined by several factors: (a) direct diffusion of ^{95}Nb atoms; (b) diffusion of ^{95}Zr isotope and its decay rate into the ^{95}Nb isotope; and (c) the decay of ^{95}Nb. All of these factors have to be taken into account to determine the ^{95}Nb diffusivity.[11] Moreover, the energies of the corresponding γ lines for the two isotopes differ by only 9 keV, which imposes relatively strong requirements on the energy resolution of the counting system.

In binary Ti aluminides, Nb diffusion can conveniently be measured by secondary ion mass spectrometry (SIMS) analysis using natural stable ^{93}Nb isotope as a tracer.[8] In this case, a thin ^{93}Nb tracer layer was deposited on the sample surface by evaporation in a vacuum chamber.

Because the SIMS analysis cannot be used in the case of ternary TiAlNb alloys, the radiotracer technique was exclusively applied in that case. In the binary Ti aluminides, the radioisotope ^{95}Nb was also applied at high temperatures to increase the temperature interval of the diffusion study and to check the consistency of the SIMS data.

2.3 Measurements of the Penetration Profiles

Conventional mechanical sectioning by grinding was performed to determine the penetration profiles of about 100 μm (or even more) in depth. Before sectioning, the diameter of each specimen was reduced by at least 1 mm to exclude any contribution of radial diffusion. The sectioning was performed with a precision grinding device.[7] The penetration depth was calculated from the loss of weight, which was determined with a microbalance after each sectioning, the diameter, and the density of each specimen.

The short penetration profiles of about 1 μm in depth were measured by ion-beam sputtering in the case of the radiotracer measurements. The sputtering device developed by Wenwer et al.[12] was used. Sputtering was performed in a high-vacuum chamber using Ar^+ ions with the energy of 1.1 keV and a beam current of 20 mA. A special mask was applied to ensure that only the central region of each sample was sputtered off. The sputtering time was converted to the respective penetration depth assuming a constant sputtering rate. The total penetration depth was calculated by measuring the crater size and the weight loss of the specimen with the known density.

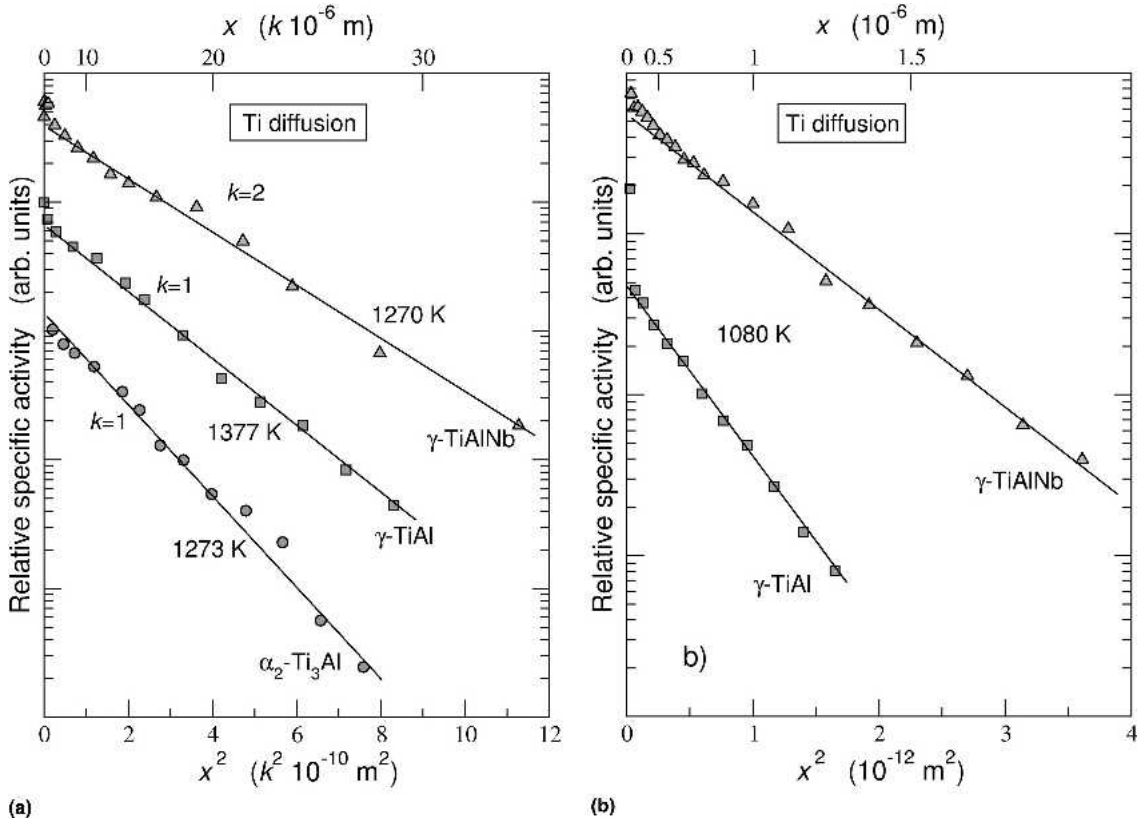

Fig. 1 Typical penetration profiles of ^{44}Ti diffusion measured by the techniques of mechanical sectioning (a) and ion-beam sputtering (b) in the Ti-33Al alloy (circles), the Ti-56Al alloy (squares), and the Ti-54Al-10Nb alloy (triangles). k is a scaling factor, and x is the penetration depth.

In-depth profiling by SIMS (CAMECA IMS-3F instrument) was performed by Dr. M. Friesel (Chalmers Technical University, Göteborg, Sweden). Nb diffusion was measured using a stable ^{93}Nb isotope. High-energy O_2^+ ions were used as the primary beam. The central area of the 200 × 200 μm^2 crater was analyzed. By assuming a constant sputter rate, the time of the analysis was converted to the penetration depth. The sputter rate was determined from the total time of the analysis and the final crater depth. The penetration profiles measured by the SIMS analysis extended to several micrometers.

3. Results

3.1 Ti Diffusion

3.1.1 High-Temperature Measurements. Typical penetration profiles measured by the mechanical sectioning technique in the Ti aluminides under consideration are presented in Fig. 1(a). A Gaussian-like distribution for the tracer was typically observed over several orders of magnitude in the decrease of the tracer concentration with the penetration depths of several tens of micrometers. The tracer diffusion coefficients D therefore were calculated from the thin layer solution of Fick's equation:

$$D = \frac{1}{4t}\left(-\frac{\partial \ln \bar{c}}{\partial x^2}\right)^{-1} \quad \text{(Eq 1)}$$

Here, $\bar{c}$ is the relative section activity (which is proportional to the tracer concentration) at depth x, and t is the diffusion time. The fits according to Eq 1 are indicated in Fig. 1 by solid lines.

3.1.2 Low-Temperature Measurements. At lower temperatures, the penetration profiles were measured by the ion-beam sputtering technique, which allows the reliable determination of short-penetration profiles (Fig. 1b) and, hence, the small diffusivities. The penetration depths, which are even smaller than 1 μm, are accessible in this case.

3.2 Nb Diffusion

Figure 2(a) represents the typical penetration profiles of Nb diffusion in the binary Ti aluminides measured by SIMS analysis. The profiles reveal the Gaussian-like behavior over several orders of magnitude in the decrease of tracer concentration.

As it is impossible to use the SIMS technique for studying Nb diffusion in the Ti-54Al-10Nb alloy, the radiotracer technique was applied throughout the whole temperature interval, as well as at several temperatures in the binary Ti-Al alloys under investigation. Two typical penetration profiles are presented in Fig. 2(b). They could be recorded up to 80 μm in depth. The profiles reveal a Gaussian type of concentration dependence over about 2 to 3 decades in the decrease of the tracer concentration.

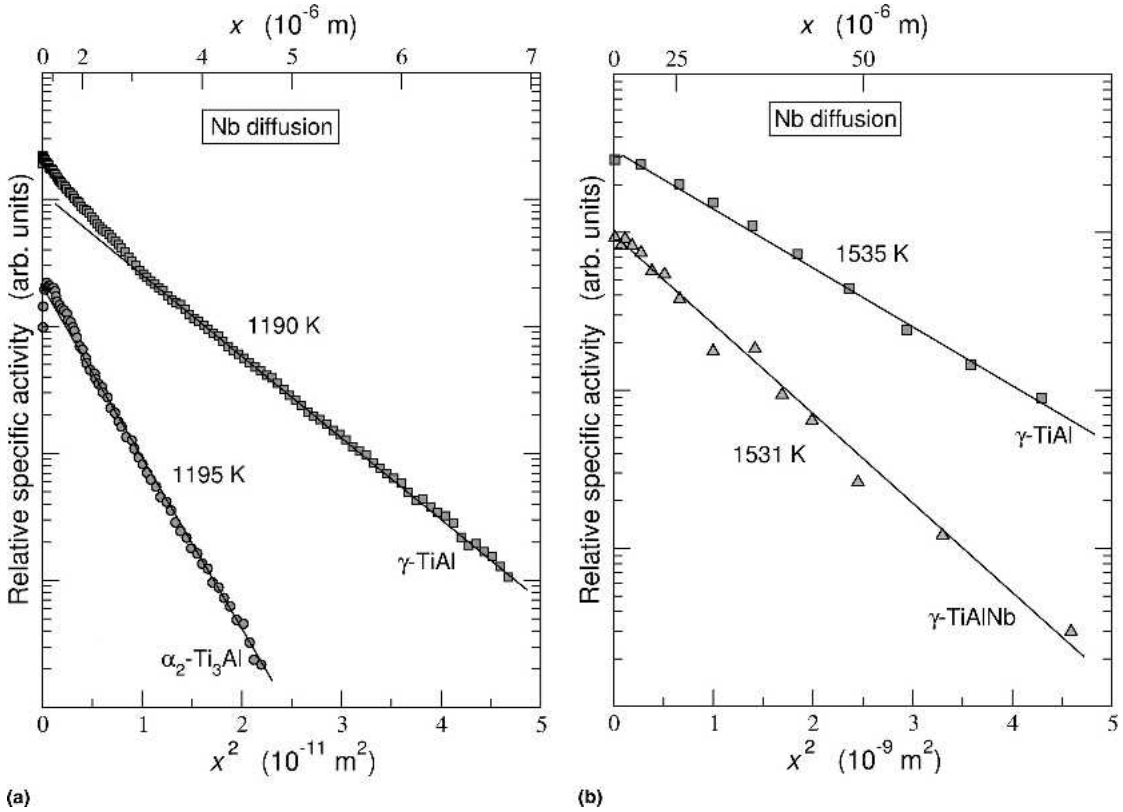

Fig. 2 Penetration profiles of Nb diffusion measured by SIMS (a) and the radiotracer technique (b) in Ti-33Al alloy (circles), Ti-56Al alloy (squares), and Ti-54Al-10Nb alloy (triangles). x is the penetration depth.

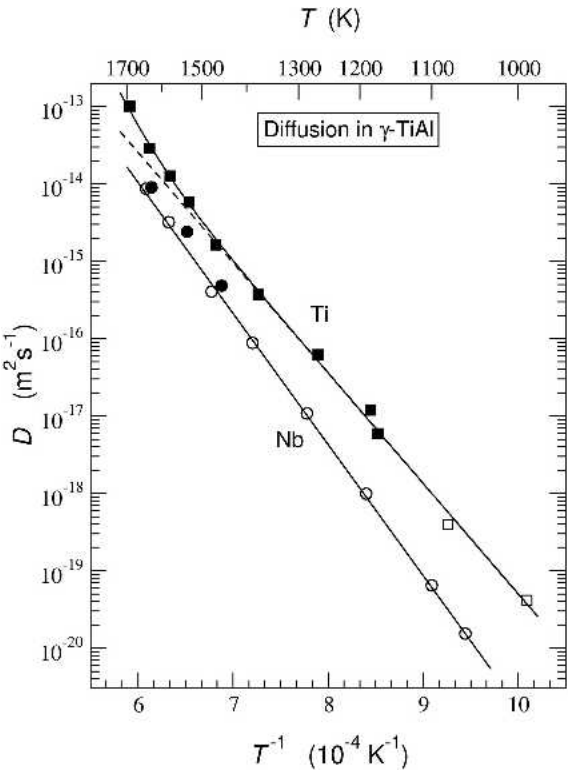

Fig. 3 Ti diffusion (squares) and Nb diffusion (circles) in the binary γTi-56Al alloy. The dashed line represents the temperature dependence of Ti diffusion, which is obtained by an Arrhenius fit at temperatures below 1470 K. The full symbols show the results of mechanical sectioning experiments,[9] whereas the open symbols represent the results of the SIMS analysis[10] and ion beam sputtering for Nb and Ti, respectively.

4. Discussion

By applying the three different techniques for the analysis of the penetration profiles, the diffusion of Ti and Nb in binary (α_2-Ti_3Al and γTiAl) and ternary γTiAl-10Nb alloys was measured in extended temperature intervals. Although quite different penetration depths were recorded, ranging from fractions of a micrometer (the ion-beam sputtering) or 5 to 10 μm (the SIMS analysis), to about 100 μm (the mechanical sectioning), consistent data were obtained. This supports the reliability of the applied procedure and the derived diffusion data.

The temperature dependence of the Ti and Nb tracer diffusion in the binary γTiAl is presented in Fig. 3. The penetration profiles for Ti diffusion were measured by mechanical sectioning at higher temperatures[9] (full squares) and by ion-beam sputtering at lower ones (open squares) (Fig. 3). The Nb diffusion was measured by the SIMS analysis[10] (open circles) and in an exemplary fashion by the radiotracer technique combined with mechanical sectioning (full circles).

While the measured diffusion coefficients of Nb can be represented by a linear Arrhenius dependence, Ti diffusion reveals strong nonlinear temperature dependence at elevated temperatures. However, below the temperature of about 1470 K the temperature dependence of the Ti diffusivity D_{Ti} can be approximated by the Arrhenius function:

$$D_{Ti} = (9.50^{+11.4}_{-5.2}) \times 10^{-6} \exp\left\{-\frac{(273.3 \pm 8)\ \text{kJ} \cdot \text{mol}}{RT}\right\} \text{m}^2/\text{s}^{-1} \quad \text{(Eq 2)}$$

Table 1 Activation enthalpy Q and preexponential factor D_0 of Ti and Nb tracer diffusion in binary and ternary titanium aluminides

Material	Tracer	D_0, m^2/s	Q, kJ/mol
α_2-Ti-33Al	Ti	2.4×10^{-5}	288
	Nb	3.2×10^{-4}	339
γ Ti-56Al	Ti	9.5×10^{-6}	273
	Nb	1.5×10^{-4}	324
γ Ti-54Al-10Nb	Ti	4.0×10^{-4}	304
	Nb	1.9×10^{-5}	280

Note: The Arrhenius parameters of Ti diffusion in the γ Ti-56Al alloy were obtained by an Arrhenius fit in the temperature range below 1470 K.

The Arrhenius parameters of Nb and Ti diffusion in the Ti aluminides under investigation are listed in Table 1.

The experimental results of Ti and Nb diffusion in the ternary high-Nb-containing γTi-54Al-10Nb alloy are presented in Fig. 4. Again, an agreement between the mechanical sectioning results and the ion-beam sputtering data is observed. Both Ni and Ti diffusivities follow Arrhenius temperature dependencies with the parameters listed in Table 1.

Nb and Ti diffusion in the binary α_2-Ti-33Al alloy were found[7,8] to follow Arrhenius temperature dependencies with the parameters given in Table 1.

Figure 5 compares the Nb and Ti diffusivities in the Ti aluminides under investigation. In all three phases, Nb diffuses more slowly than Ti. This difference amounts to about an order of magnitude in the binary α_2-Ti-33Al and γTi-56Al phases. Simultaneously, the activation enthalpy of Nb diffusion Q_{Nb} is considerably larger than that of Ti diffusion, Q_{Ti}, by almost 50 kJ/mol in these phases (Table 1). In the ternary γTi-54Al-10Nb alloy, Nb diffuses more slowly than Ti only by a factor of two to three. The two activation enthalpies, Q_{Nb} and Q_{Ti}, are quite similar in the high-Nb-containing alloy.

The ordered lattice structures of the binary γTiAl and α_2-Ti_3Al phases are schematically presented in Fig. 6. The ternary high-Nb-containing γTi-54Al-10Nb alloy also has a layered $L1_0$ structure (Fig. 6b).

Nb was shown to occupy the Ti sublattice in both α_2-Ti_3Al[13] and γTiAl.[14,15] In a ternary γTiAlNb alloy, the Nb atoms hence occupy the Ti sublattice dominantly. Heavy Nb alloying of the γTiAl intermetallics increases both parameters a and c of the $L1_0$ structure as well as their ratio c/a.[15]

One of the most striking features in Fig. 3 is a strongly curved temperature dependence of Ti diffusion in γTiAl, if it is measured in an extended temperature interval.[9] This

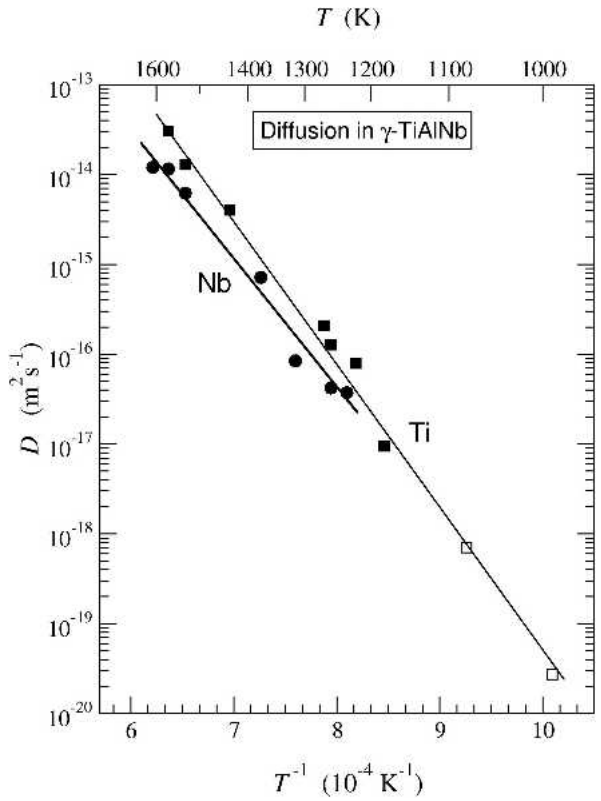

Fig. 4 Arrhenius plot of Ti diffusion (squares) and Nb diffusion (circles) in the ternary γTi-54Al-10Nb alloy. The full symbols show the results of mechanical sectioning experiments, whereas the open symbols represent the results obtained by ion beam sputtering.

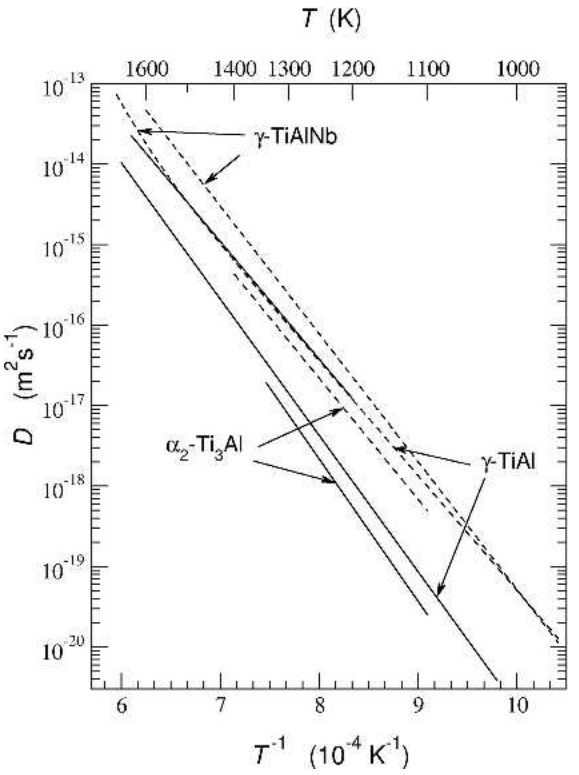

Fig. 5 Ti diffusion (dashed lines) and Nb diffusion (full lines) in the γTi-54Al-10Nb ternary alloy in comparison to their diffusivities in the binary γTi-56Al alloy[9,10] and α_2-Ti-33Al alloy[7,8]

behavior was explained by accounting for different atomistic mechanisms of Ti diffusion at lower and higher temperatures in γTiAl.[9,16] According to atomistic calculations, the vacancy concentration on the Ti sublattice exceeds that on the Al sublattice by orders of magnitude.[9] Moreover, a relatively high concentration of Ti antistructure atoms (i.e., Ti atoms on Al sublattice in antistructure positions) was calculated to be formed, especially at higher temperatures.[9] Whereas the Ti sublattice diffusion mechanism was proposed to dominate Ti diffusion at lower temperatures, the so-called antistructure bridge mechanism benefits from the large concentration of Ti antistructure atoms and enhances significantly the Ti diffusivity at higher temperatures.[9] On the other hand, a linear temperature dependence of Ti diffusion in α_2-Ti_3Al was observed when plotted in the Arrhenius coordinates[7] (Fig. 5). This behavior was related to the Ti sublattice diffusion mechanism in the $D0_{19}$ structure (Fig. 6a) of the α_2-Ti_3Al alloy.[7]

As mentioned above, Nb diffuses more slowly than Ti in the binary α_2-Ti_3Al and γTiAl aluminides by an order of magnitude. Due to the preferential solubility of Nb to the Ti sublattice,[14] such behavior was explained by the Ti sublattice diffusion mechanism of Nb atoms and a repulsive interaction between Nb atoms and Ti vacancies. According to the standard electrostatic model of vacancy-solute atom interaction,[17] one would expect that the addition of Nb to TiAl would produce a retardation effect on the diffusion rates. This is definitely not the case for the high-Nb-containing alloys. Both Ti and Nb diffuse faster in the ternary alloy in comparison to the binary ones.

Because the addition of a large amount of Nb atoms increases both the lattice parameters and the *c*/*a* ratio,[15] the energy barriers may be decreased, enhancing simultaneously the diffusion rates. Atomistic simulations would be helpful to explain the observed experimental behavior.

Heavy alloying by Nb was shown to enhance the creep resistance of TiAl alloys at working temperatures of about 700 °C.[2] Extrapolating the Ti diffusivity in the ternary γTi-54Al-10Nb and the binary γTi-56Al alloys down to these temperatures, one can see that the ratio of the diffusion rates is reversed: self-diffusion in γTiAl alloy occurs faster than in the ternary γTiAlNb alloy (Fig. 5).

The above-mentioned superior creep properties of Ti-Al-Nb alloys may probably be related to this bulk diffusion retardation. However, one should not overinterpret this finding. At relatively low working temperatures, grain boundary diffusion may play a decisive role and may profoundly affect the creep resistance. In this case, the probable segregation of Nb atoms at grain boundaries can produce a retardation effect on the grain-boundary self-diffusion of Ti and thus on the creep rate.

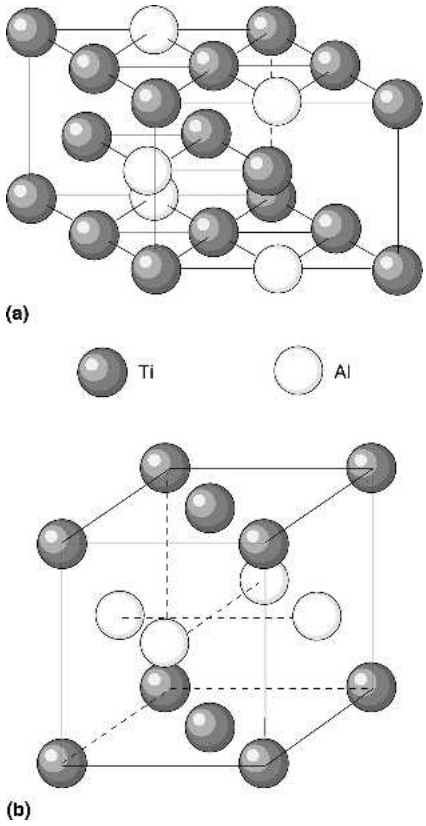

Fig. 6 The $D0_{19}$ (a) and $L1_0$ (b) lattice structures of the α_2-Ti_3Al and γTiAl phases, respectively

5. Summary

Ti and Nb tracer diffusion in the binary alloys (α_2-Ti-33Al and γTi-56Al) and ternary γTi–54Al-10Nb alloy is presented. The results obtained by the mechanical sectioning (larger penetration depths >10 μm and higher temperatures) are very consistent with the diffusion data derived by ion-beam sputtering or SIMS analysis (i.e., shorter penetration depths of several micrometers or even less, and lower temperatures). This supports the reliability of the diffusion data that were determined.

Both Ti and Nb reveal almost linear Arrhenius-type temperature dependencies in all phases, excepting the case of Ti diffusion in γTiAl. In the latter case, a strongly curved temperature dependence is obtained. In the temperature interval studied, Nb diffuses more slowly than Ti by an order of magnitude in the two binary aluminides and by a factor of two to three in the ternary high-Nb-containing alloy.

Both Ti and Nb tracer diffusivities are enhanced in the ternary composition with respect to their diffusivities in binary Ti_3Al and TiAl alloys at $T > 1000$ K. The effect is related to an elastic distortion of the $L1_0$ structure of the γTiAl phase by alloying with oversized Nb atoms.

Acknowledgments

The authors thank Dr. F. Appel and Dr. J.D.H. Paul (GKSS Research Center) for the preparation of the Ti-54Al-10Nb alloy and for valuable discussion. The authors are indebted to Dr. M. Friesel (Chalmers Technical University, Göteborg, Sweden) for performing the SIMS analyses of the alloys.

References

1. F. Appel, J.D.H. Paul, M. Oehring, U. Frobel, and U. Lorenz, Creep Behaviour of TiAl Alloys with Enhanced High-Temperature Capability, *Metall. Mater. Trans. A,* Vol 34, 2003, p 2149-2164
2. F. Appel, J.D.H. Paul, M. Oehring, H. Clemens, and F.D. Fischer, Physical Metallurgy of High Nb-Containing TiAl Alloys, *Z. Metallkd.,* Vol 95, 2004, p 585-591
3. J.W. Fergus, Effect of Niobium Additions on CO_2-Enhanced Oxidation of Titanium-Aluminium Intermetallic Alloys. *Oxid. Metall.,* Vol 48, 1997, p 201-214
4. G.L. Chen, Z.Q. Sun, and Z. Xing, Oxidation and Mechanical-Behaviour of Intermetallic Alloys in the Ti-Nb-Al Ternary-System, *Mater. Sci. Eng. A,* Vol 153, 1992, p 597-601
5. F. Appel, M. Oehring, J.D.H. Paul, C. Klinkenberg, and T. Carneiro, Physical Aspects of Hot-Working Gamma-Based Titanium Aluminides, *Intermetallics,* Vol 12, 2004, p 791-802
6. A. Hellwig, M. Palm, and G. Inden, Phase Equilibria in the Al-Nb-Ti System at High Temperatures, *Intermetallics,* Vol 6, 1998, p 79-94
7. J. Rüsing and C. Herzig, Concentration and Temperature Dependence of Titanium Self-Diffusion and Interdiffusion in the Intermetallic Phase Ti_3Al, *Intermetallics,* Vol 4, 1996, p 647-657
8. J. Breuer, T. Wilger, M. Friesel, and C. Herzig, Interstitial and Substitutional Diffusion of Metallic Solutes in Ti_3Al, *Intermetallics,* Vol 7, 1999, p 381-388
9. C. Herzig, T. Przeorski, and Y. Mishin, Self-Diffusion in Gamma-TiAl: An Experimental Study and Atomistic Calculations, *Intermetallics,* Vol 7, 1999, p 389-404
10. C. Herzig, T. Przeorski, M. Friesel, F. Hisker, and S.V. Divinski, Tracer Solute Diffusion of Nb, Zr, Cr, Fe, and Ni in Gamma-TiAl: Effect of Preferential Site Occupation, *Intermetallics,* Vol 9, 2001, p 461-472
11. C. Herzig, U. Köhler, and S.V. Divinski, Tracer Diffusion and Mechanism of Non-Arrhenius Diffusion Behaviour of Zr and Nb in Body-Centred Cubic Zr-Nb Alloys, *J. Appl. Phys.,* Vol 85, 1999, p 8119-8130
12. F. Wenwer, A. Gude, G. Rummel, M. Eggersmann, T. Zumkley, N.A. Stolwijk, and H. Mehrer, A Universal Ion-Beam-Sputtering Device for Diffusion Studies, *Meas. Sci. Technol.,* Vol 7, 1996, p 632-640
13. D.G. Konitzer, I.P. Jones, and H.L. Fraser, Site Occupancy in Solid-Solutions of Nb in the Intermetallic Compounds TiAl and Ti_3Al. *Scr. Metall.,* Vol 20, 1986, p 265-268
14. Y.L. Hao, D.S. Xu, Y.Y. Cui, R. Yang, and D. Li, The Site Occupancies of Alloying Elements in TiAl and Ti_3Al Alloys, *Acta Mater.,* Vol 47, 1999, p 1129-1139
15. H. Erschbaumer, R. Podloucky, P. Rogl, G. Temnitschka, and R. Wagner, Atomic Modeling of Nb, V, Cr, and Mn Substitutions in Gamma-TiAl: 1—c/a-Ratio and Site Preference, *Intermetallics,* Vol 1, 1993, p 99-106
16. Y. Mishin and C. Herzig, Diffusion in the Ti-Al System, *Acta Mater.*, Vol 48, 2000, p 589-623
17. A.D. Le Claire, Solute Diffusion in Dilute Alloys, *J. Nucl. Mater.,* Vol 69/70, 1978, p 70-96